Convective isolation of Hadean mantle reservoirs through Archean time

Jonas Tusch[1], Carsten Münker[1], Eric Hasenstab[1], Mike Jansen[1], Chris S. Marien[1], Florian Kurzweil[1], Martin J. Van Kranendonk[2], Hugh Smithies[3], Wolfgang Maier[4], Dieter Garbe-Schönberg[5]

[1]Institut für Geologie und Mineralogie, Universität zu Köln, Zülpicher Str. 49b, 50674 Cologne, Germany
[2]School of Biological, Earth and Environmental Sciences, and Australian Center for Astrobiology, The University of New South Wales, Kensington, NSW, 2052, Australia
[3]Geological Survey of Western Australia, Mineral House, 100 Plain Street, East Perth, WA 6004, Australia
[4]School of Earth and Ocean Sciences, Cardiff University, Cardiff, UK
[5]Institut für Geowissenschaften, Universität zu Kiel, Ludewig-Meyn-Str. 2-6, 24118 Kiel, Germany

ABSTRACT

Although Earth has a convecting mantle, ancient mantle reservoirs that formed within the first hundred Ma of Earth's history (Hadean Eon) appear to have been preserved through geologic time. Evidence for this is based on small anomalies of isotopes such as ^{182}W, ^{142}Nd and ^{129}Xe that are decay products of short-lived nuclide systems. Studies of such short-lived isotopes have typically focused on geological units with a limited age range and therefore only provide snapshots of regional mantle heterogeneities. Here we present for the first time a dataset for short-lived ^{182}Hf-^{182}W (half-life 9Ma) in a comprehensive rock suite from the Pilbara Craton, Western-Australia. The samples analyzed, preserve a unique geological archive covering 800 Ma of Archean history. Pristine ^{182}W signatures that directly reflect the W isotopic composition of parental sources are only preserved in unaltered mafic samples with near canonical W/Th (0.07-0.26). Early Paleoarchean , mafic igneous rocks from the East-Pilbara Terrane display a uniform pristine μ^{182}W excess of 12.6±1.4 ppm. From ca. 3.3Ga onwards, the pristine^{182}W signatures progressively vanish and are only preserved in younger rocks of the craton that tap stabilized ancient lithosphere. Given that the anomalous ^{182}W signature must have formed by ca. 4.5Ga, the mantle domain that was tapped by magmatism in the Pilbara Craton must have been convectively isolated for nearly 1.2Ga. This finding puts lower bounds on timescale estimates for localized convective homogenization in early Earth's interior and on the widespread emergence of plate tectonics that are important input parameters in many physical models.

Significance Statement

Geological processes like mantle convection or plate tectonics are an essential factor controlling Earth's habitability. Our study provides new insights into timescales of convective homogenization of Earth's early mantle, employing the novel tool of high precision 182W isotope measurements to rocks from the Pilbara craton in Australia, spanning an age range from 3.5 to 2.7 billion years. Previous ^{182}W studies mostly covered snapshots through geologic time, so the long-term ^{182}W-evolution of the mantle has been ambiguous. Together with

sophisticated trace element approaches, we can now provide an improved insight into such timescales, arguing for local preservation of primordial geochemical heterogeneities within Earth's mantle as late as around 3.0 billion years, the putative onset of widespread plate tectonics on Earth.

Among the terrestrial planets, Earth is unique in that plate tectonic processes efficiently mix and homogenize its silicate mantle. Surprisingly, however, geochemical studies have revealed that both Archean and Phanerozoic mantle reservoirs still carry primordial geochemical signatures, thus escaping efficient convective homogenization as also predicted by geodynamic models(1, 2). The main evidence for such ancient geochemical heterogeneities stems from noble gas systematics(3) and from short-lived nuclide decay-series that became extinct after the Hadean eon (>4.0 Ga)(4, 5). For instance, the relative abundance of daughter isotopes from short-lived nuclide-series such as ^{142}Nd and ^{182}W show significant variations in ancient rocks when compared to the Earth's modern mantle composition(4, 5). From these short-lived isotope systems, the ^{182}Hf – ^{182}W decay system has proven particularly useful in constraining the timing of planetary core formation(6), timescales of late accretion, and silicate differentiation(7, 8).

There are two competing explanations for the origin of ^{182}W isotope anomalies found in the terrestrial rock record, arising from the markedly different geochemical behavior of Hf and W during both core formation and silicate differentiation in planetary bodies. As primitive meteorites exhibit strong ^{182}W isotope deficits (μ^{182}W = -190)(6), the observation of positive ^{182}W anomalies in Eoarchean rocks was interpreted as evidence that these rocks lacked a late veneer component(5). Conversely, the presence of some late accreted material is required to explain the elevated abundances of highly siderophile elements (HSE) in Earth's modern silicate mantle(9). Notably, some Archean rocks with apparent pre-late veneer like ^{182}W isotope excesses were shown to display HSE concentrations that are indistinguishable from modern mantle abundances(10), which is difficult to reconcile with the missing late veneer hypothesis. An alternative suggestion is therefore that early silicate differentiation during the lifetime of ^{182}Hf might have caused the formation of mantle reservoirs with anomalous ^{182}W signatures(10, 11). In addition, recent studies have revealed variable ^{182}W isotope deficits in the mantle plume sources of ocean island basalts (OIBs)(12). In line with noble gas systematics and seismic properties of such deep-rooted mantle plumes, these ^{182}W deficits have been taken as evidence for the presence of primordial domains that have been convectively isolated since Earth's earliest history(12). The origin of this modern igneous reservoir remains ambiguous (13–15) and its presence in pre-Phanerozoic time is highly speculative. However, the contribution of modern mantle plume sources with ^{182}W deficits to the convecting mantle offers an additional explanation for the decrease of ^{182}W isotope excesses since the Archean as a consequence of increasing mantle homogenization (see SI Appendix).

Surprisingly few studies have directly assessed the ^{182}W record of mantle-derived rock assemblages that span a relatively long time frame of Archean geodynamic evolution. Arguably, there already are comprehensive studies from the Slave Craton(16), SW Greenland(11, 17), and Southern Africa(18) that investigated lithostratigraphic successions covering time series of several hundred million years. However, these studies only covered crustal reservoirs (TTGs and diamictites) but not mafic rocks that allow direct tracing of mantle-derived magmatic pulses. Notably, fluid mobility of W already may have caused significant disturbance of primary ^{182}W isotope systematics in hydrated mafic precursors of such previously investigated TTG suites(16, 19, 20). Hence, W/Th ratios of TTGs may not necessarily reflect the primary W/Th ratios of their mafic precursors. In fact, subcanonical W/Th ratios are often observed in TTGs(e.g. 19), that may reflect (i) preferential loss of W during dehydration at amphibolite facies conditions prior to partial anataxis or (ii) preferential retention

of W in residual rutile(22). It is therefore more than plausible that apparently invariant ^{182}W isotope excesses in felsic crustal assemblages(16) may simply mirror fluid-mediated W redistribution within their hydrated mafic precursors(19, 20) obscuring primary magmatic trends. Moreover, ^{182}W studies on sediments like glacial diamictites only provide average crustal compositions and protracted information on convective processes in the mantle. An exceptional case in this regard are studies from SW Greenland(5, 11, 17). These 3.8-3.4 Ga old mantle-derived rocks from SW Greenland show uniform ^{182}W excesses but decreasing ^{142}Nd anomalies through time in the same lithostratigraphic successions(11, 17). This relationship suggests that an original decrease in ^{182}W was obscured by secondary W redistribution during metamorphism(17), as also suggested for Archean rocks from the Acasta Gneiss Complex(23), from the North Atlantic Craton(24) and from the Superior Province(25). Collectively, these examples illustrate that most studies have only provided snapshots of the ^{182}W isotope evolution of the mantle beneath individual Archean cratons (see SI Appendix) and that robust information on the ^{182}W isotope evolution of the Archean mantle with time is scarce and often ambiguous due to secondary disturbance. In fact, only 15 percent of all available samples previously analyzed for ^{182}W display W abundances that are pristine with respect to an unmodified mantle source (see SI Appendix). In order to allow for a more comprehensive understanding of Archean geodynamic evolution, studies are required to assess the ^{182}W isotope evolution of a particular region over a long time period, with a focus on mantle-derived rocks.

Here we present for the first time a nearly continuous ^{182}W isotope record for an Archean craton that spans an age range of 800 Ma, from the Paleo- to the Neoarchean and covers both mafic and felsic compositions. We investigated the ^{182}W isotope evolution of the exceptionally well preserved 3.58 – 2.76 Ga old Pilbara Craton (Western Australia). Since much of this craton is only little affected by metamorphism(26), many units within the lithostratigraphic successions are more likely to have preserved their primary W systematics than other more deformed cratons of similar age. Therefore, our new data may allow a much more robust assessment of ^{182}W isotope evolution through the Archean. A detailed outline of the geologic evolution of the Pilbara Craton is provided in the SI Appendix. In short, mantle-derived (mafic and ultramafic) magmatic sequences in the east [East Pilbara Terrane (EPT); Warrawoona, Kelly, and Sulphur Springs groups] and west [West Pilbara Superterrane (WPS); Ruth Well Formation] of the craton cover an age range from 3.52 – 3.23 Ga and tapped rather depleted mantle sources that were emplaced during distinct mantle plume events, similar to modern plateau basalts(27, 28). Burial of these mafic sequences, together with older protocrust, caused melting to form four supersuites of sodic (tonalites, trondhjemites and granodiorites) and potassic granitoids (granites) that can be regarded as probes of early mafic crust. The younger evolution of the EPT involved plume-initiated rifting (Soanesville Group) at 3.18 Ga and subsequent accretion (3.07 Ga) of the younger WPS that also includes ~3.1 Ga subduction related mafic lithologies (Whundo Group)(29, 30). After amalgamation, post-orogenic, lithosphere-derived magmatism included mafic rocks from the Bookingarra Group (Opaline Well Intrusion, Louden -, and Mount Negri Volcanics) and crust-derived post-tectonic granites (e.g., Split Rock Supersuite)(26).

We employed two strategies in selecting our samples. Firstly, we analyzed mafic volcanic rocks that tapped the ambient asthenospheric mantle of the EPT (plume-derived) and the WPS (subduction related). Secondly, to understand the evolution of the lithosphere and to obtain average crustal compositions we analyzed mafic dikes, sediments and granitoids of different ages. We studied a total of 56 samples from more than ten major stratigraphic units of the two different terranes (SI Appendix, Fig. S1), also covering different tectonic regimes (vertical tectonics in the EPT and horizontal tectonics in the WPS). For all these samples, selected trace element abundances (Zr, Nb, Ta, W, Th & U) were obtained by isotope dilution measurements (details in the SI Appendix). Ten ultramafic (komatiite) samples were also previously analyzed for HSE(31). High-precision W isotope measurements were performed on a subset of 30 samples. We followed a slightly modified analytical protocol of reference (17) as outlined in the SI Appendix. Results of high-precision W isotope analyses are reported in

the μ-notation (equivalent to ppm) relative to NIST SRM 3163 and given in Datasets S1 (session mean values) and S2 (single measurements). The $\mu^{182}W$ isotope compositions addressed in this manuscript always refer to the measured $^{182}W/^{184}W$ ratio that has been corrected for mass bias by using $^{186}W/^{184}W = 0.92767$ (denoted `6/4´)(32). Major- and trace-element composition and isotope dilution measurements are reported in Dataset S3.

High-precision concentration measurements are required to identify samples with primary W abundances, because W is strongly fluid-mobile when compared to elements of similar incompatibility (e.g. Th, U, Ta)(33). Thus, W mobility during fluid alteration results in non-canonical W/Th ratios(33) whereas in undisturbed magmatic systems, the similarly high incompatibility of W and Th results in canonical W/Th ratios between 0.09 and 0.24 over a wide range of mafic to felsic melts(33). Our Archean rock samples display primary magmatic trends for Th versus Zr (Fig. 1a), but not for W versus Zr, as W was enriched in many samples (Fig. 1b). Samples with canonical W/Th ratios, however, define a pristine magmatic trend (Fig. 1b) allowing us to restrict further consideration primarily to samples with ^{182}W isotope composition unmodified by secondary processes.

The oldest plume-related mafic volcanic samples from the EPT (Warrawoona Group) all display resolvable ^{182}W excesses. However, Warrawoona Group rocks, and a slightly older gabbroic enclave from the Shaw Granitic Complex (Mount Webber Gabbro; Pil17-07), with supracanonical W/Th ratios, display markedly lower $\mu^{182}W$ compositions when compared to samples with undisturbed elemental W budgets. Samples with primary W concentrations (canonical W/Th) display an average of $\mu^{182}W = +12.6 \pm 1.4$ ppm [95% confidence interval (CI), n=8, also including previously published data for two samples from the Apex basalt(14), red bar in Fig. 2], whereas rocks affected by secondary W-enrichment display a resolvably lower excess of ~ +8.1 ± 1.4 ppm (95% CI, n=8; grey bar in Fig. 2). Interestingly, the average ^{182}W excess in the metasomatized samples is indistinguishable from the long-term lithospheric average (see Fig. 2 and below). Samples from the younger, plume-derived ~3.35 Ga Kelly Group (Euro Basalt) exhibit a contrasting pattern. The altered sample Pil16-39a displays a $\mu^{182}W$ value of +8.5 ± 2.1 ppm, again indistinguishable from the long-term lithospheric average. However, the unaltered sample Pil16-53a shows a resolvably lower excess of $\mu^{182}W = +5.2 \pm 2.6$ ppm when compared to unaltered samples from the Warrawoona Group. The youngest sample from the EPT, a 3.18 Ga Honeyeater basalt, displays no ^{182}W isotope excess, overlapping the modern upper mantle value (Pil16-51, $\mu^{182}W = +1.1 \pm 3.9$ ppm). The eruption of the Honeyeater Basalt marks extension at the onset of clear plate tectonic style processes (the earliest recorded Wilson Cycle) in the Pilbara Craton(30). Thus, decreasing $\mu^{182}W$ values in the unaltered samples indicate a diminishing ^{182}W isotope excess with time during a change in the tectonic regime. Additional evidence for change in geodynamic pattern is manifested in rocks from the 3.13-3.11 Ga Whundo Group (WPS), a sequence with geochemical characteristics that are consistent with derivation from a depleted mantle source that was variably affected by subduction components in an arc-like setting(29). Samples from the Whundo Group exhibit consistently lower $\mu^{182}W$ (Pil16-67: $\mu^{182}W = +5.3 \pm 4.8$ and Pil16-74: $\mu^{182}W = +5.9 \pm 3.2$) than Warrawoona Group samples with canonical W/Th ratios. Beside data for 3.48 Ga komatiites from the Komati Formation of the Kapvaal Craton(10), our data provide the oldest evidence for modern upper mantle-like W isotope compositions in the early Archean rock record.

The ^{182}W isotope excesses also slightly decrease in granitoids: Sodic and potassic granitoids (Pil16-34 and Pil16-35, 3.47 Ga North Shaw Tonalite and Pil16-41, 3.47 Ga Homeward Bound Granite) display $\mu^{182}W$ values that are indistinguishable from the Warrawoona Group average (only considering samples with canonical W/Th ratios). However, highly fractionated post-orogenic monzogranites (Pil16-36A, 2.85 Ga Spearhill Monzogranite and Pil16-12, 3.45 Ga North Pole Monzogranite; blue squares in Fig. 2) display significantly lower $\mu^{182}W$ values as this Warrawoona Group average. Hence, the granitoids in the EPS mimic the ^{182}W isotopic evolution of the ambient mantle, although with some delay. Given that the oldest and less evolved sodic granites are directly derived from mafic protocrust, this protocrust must have had an average ^{182}W excess similar to that of the Warrawoona Group samples. Lower ^{182}W

isotope excesses in younger and more evolved granitoids mirror the temporal decrease in ^{182}W as also observed for mantle-derived mafic rocks. Prevalent ^{182}W excesses that are lower than the pristine Warrawoona Group average (canonical (W/Th) are also recorded in Meso- to Neoarchean shales (Pil16-50B, 3.19 Ga Paddy Market Formation and Pil16-38b, 2.76 Ga Hardey Formation, $\mu^{182}W$ between +7.1 and +7.6 ppm), a rift-related lithosphere-derived dolerite from the Fortescue Group ($\mu^{182}W$ = +7.6 ± 3.1 ppm Pil16-31, 2.78 Ga Black Range dolerite) and mafic rocks from the Bookingarra Group (ca. 2.95 Ga; Pil16-63, -65 & -75), which derived from a metasomatized, lithospheric mantle source that was refertilized by subducted sediments in a subduction zone-like setting(34) ($\mu^{182}W$ between +8 and +11 ppm; Fig. 2). The shales provide an average of the ^{182}W isotope composition of the upper crust, and the lithosphere-derived mafic intrusion probes the composition of the subcontinental lithospheric keel. Unlike the shales, a Paleoarchean Algoma-type Banded Iron Formation (BIF) from the EPT (Pil16-62B, 3.47 Ga Duffer Formation) has negligible detrital components (0.4% Al_2O_3), and carries a ^{182}W excess of +9.0 ± 3.3 ppm. We interpret this signature as being seawater-derived and reflecting the average composition of the ambient hydrothermal input provided by local volcanism with similar W isotope composition.

Altogether, the integrated ^{182}W isotope compositions recorded in granitoids, shales and lithosphere-derived rocks provide a lithospheric average $\mu^{182}W$ of +8.3 ± 1.0 ppm (N = 11, blue bar in Fig. 2), which is significantly lower than the average $\mu^{182}W$ of +12.6 ± 1.4 ppm for Warrawoona Group samples with canonical W/Th (N = 8, red bar in Fig. 2) but higher than the modern upper mantle-like $\mu^{182}W$ of +1.1 ± 3.9 ppm for the Honeyeater Basalt. Thus, the lithospheric average seems to record the integrated ^{182}W isotope composition of different mantle reservoirs. Samples from the EPT that were affected by secondary W enrichment (grey bar in Fig. 2) show a similar average as the lithosphere-derived rocks, which is evidence for a craton wide homogenization of ambient ^{182}W isotope compositions and the partial homogenization of primary ^{182}W isotope variability. Hence, using elemental W-Th systematics is a key tool, as this can unambiguously clarify the origin of ^{182}W isotope variability. In contrast to a previous study(35), where this tool has not been applied and altered samples were studied, we can now distinguish between diminishing ^{182}W isotope anomalies in the ambient mantle and secondary processes that re-distribute ^{182}W isotope anomalies (Fig. 1c).

Our study demonstrates that the oldest mantle-derived rocks from the Pilbara Craton with canonical W/Th display ^{182}W isotope excesses of a magnitude similar to other Archean cratons. As outlined above, however, there is no uniformly accepted explanation for the origin of these ^{182}W excesses. For the Pilbara Craton, the missing late veneer hypothesis provides a plausible explanation, as decreasing depletions of Platinum Group Elements (PGE) in komatiites with decreasing age are consistent with a progressive in-mixing of late veneer material(31). Amongst the ten komatiite samples from the EPT and WPS that were previously analyzed for HSE(31) we found only one sample (179738) that preserved its primary W budget. All other komatiites from this sample selection were metasomatically overprinted and exhibit strongly elevated W/Th ratios exceeding 51 (sample 160245). This confirms previous evidence that ultramafic rocks are extremely susceptible to (fluid mediated) second stage enrichment of W(17), which causes decoupling of HSE and ^{182}W systematics. The komatiite sample 179738 (3.46 Ga Apex Basalt of the Warrawoona Group) with a canonical W/Th ratio is strongly depleted in PGE(36) and displays an elevated ^{182}W of +11.9 ± 2.9 ppm, consistent with a model assuming an incomplete late veneer contribution to the mantle source of this sample. Such an interpretation is also in line with the absence of ^{142}Nd anomalies in Pilbara rock samples that show significant PGE depletions(35), thereby negating early silicate crystal-liquid differentiation as an additional explanation for the occurrence of ^{182}W isotope excesses in the Pilbara samples. Collectively, our data indicate that Hadean, pre-late veneer mantle was preserved in the mantle sources of Pilbara igneous rocks until ca. 3.3-3.1 Ga, much longer than evident from other cratons(11, 25). The long-standing apparent mismatch between virtually constant ^{182}W isotope excesses and progressively vanishing ^{142}Nd anomalies through Archean time(11) is therefore well explained by the larger mobility of W compared to Nd and its re-distribution during secondary processes. By only considering samples with strictly canonical W/Th ratios, we show that the prevalence of ^{182}W isotope excesses even in the

younger Archean rock record (Fig. 3) may be a vestige of older rocks, from which W was progressively redistributed. Hence, we rather argue that mantle convection homogenized primordial ^{182}W isotope anomalies during the Paleo- and Mesoarchean (Fig. 3) at the same timescales as ^{142}Nd systematics(37).

Our ^{182}W results for the Pilbara Craton have important implications for understanding timescales of geodynamic processes on the early Earth and provide a future reference parameter for geodynamic models addressing mantle mixing in the early Earth. Geodynamic models addressing the Pilbara data have to account for the observations that (1) a Hadean pre-late veneer signature remains isolated for over more than 1 billion years and (2) such an isotopically isolated mantle domain continuously triggered prolonged plume-driven magmatism with a distinct isotopic signature, most likely in a stagnant lid regime(38). In contrast to present-day mantle plumes with negative ^{182}W signatures(12), Archean mantle plumes beneath the Pilbara Craton appear to have carried rather uniform ^{182}W isotope excesses that were similar to the shallower mantle, thus arguing that compositionally distinct deep mantle sources such as large low-shear velocity provinces (LLSVPs) or ultra-low velocity zones (ULVZs) may not have been involved or, alternatively, even may not have formed(38, 39).

The marked geodynamic transition at 3.3 – 3.1 Ga in the Pilbara Craton with influx of modern-like, upper mantle material with smaller ^{182}W isotope excesses coincides with models claiming a global transition from stagnant lid-type regimes towards modern plate tectonics. This transition is, for instance, postulated from crustal growth curves based on the zircon record(40), from the increased occurrence of subduction-like magmatism in the Archean(41), the change of composition in the subcontinental lithospheric mantle(42), and from increasingly larger volumes of exposed felsic crust(43). It is therefore tempting to postulate that the initiation of plate tectonics caused a more efficient homogenization of Earth's mantle than vertical, plume-driven dynamics that prevailed in a stagnant lid regime as proposed for the older units of the Pilbara Craton. Indeed, geodynamic models for a stagnant lid regime show that, contrary to expectation, the timescales of mantle mixing in the Archean were not accelerated due to a hotter thermal state of the mantle but were rather prolonged(37). The Archean regime was possibly characterized by small, isolated convection cells and episodic mantle overturn events that vertically homogenized discrete regions of the mantle(38, 44) but maintained lateral heterogeneities for billions of years(2). Most likely, the initiation of modern plate tectonics was not a sudden event but rather occurred gradually(45). These circumstances might explain why (i) other Archean lithostratigraphic successions of similar age as the Pilbara Craton display invariant ^{182}W patterns(16, 23) or already show modern upper mantle-like $\mu^{182}W$ isotope compositions (10) and (ii) why in some cases ^{182}W anomalies survived at least until the late Archean(46). In fact, our interpretation is in line with a recent study interpreting heterogeneous ^{182}W isotope compositions in Archean rocks as expressing localized subduction events (as in the Pilbara Craton) during a transition period (~3.6 to 2.7 Ga) from plume tectonics to modern plate tectonics(47).

In summary, our study demonstrates that the Pilbara Craton preserved a natural laboratory for studying Archean geodynamics that may serve as a future test case for interdisciplinary studies assessing timescales of mantle dynamics through deep time. Complementary to attempts inferring timescale estimates for mantle stirring times from global modelling(48) our approach adds to a more detailed information pattern providing individual homogenization histories of isotopically anomalous Archean mantle domains. Therefore, the rock record of the Pilbara Craton provides important observational constraints on convective processes within the Archean mantle which are indispensable for numerical simulations as such input parameters define the evolutionary pathway of computational convection models(49).

Competing interest statement

The authors declare no competing interest.

Acknowledgments

This research was funded by the German Research Foundation (DFG, grant no. MU 1406/18-1) to C. Münker as part of the priority program 1833 *"Building a Habitable Earth"*. MVK is supported by the Australian Research Council through Discovery Project DP180103204. HS publishes with the permission of the Executive Director, Geological Survey of Western Australia. We thank Frank Wombacher for maintenance of the MC-ICP-MS and for managing the clean-lab. We are grateful to Alessandro Bragagni, Frank Wombacher and Mario Fischer-Gödde for helpful discussions concerning analytical issues. Comments by two anonymous reviewers and the editor helped to improve the manuscript.

Figures

Fig. 1

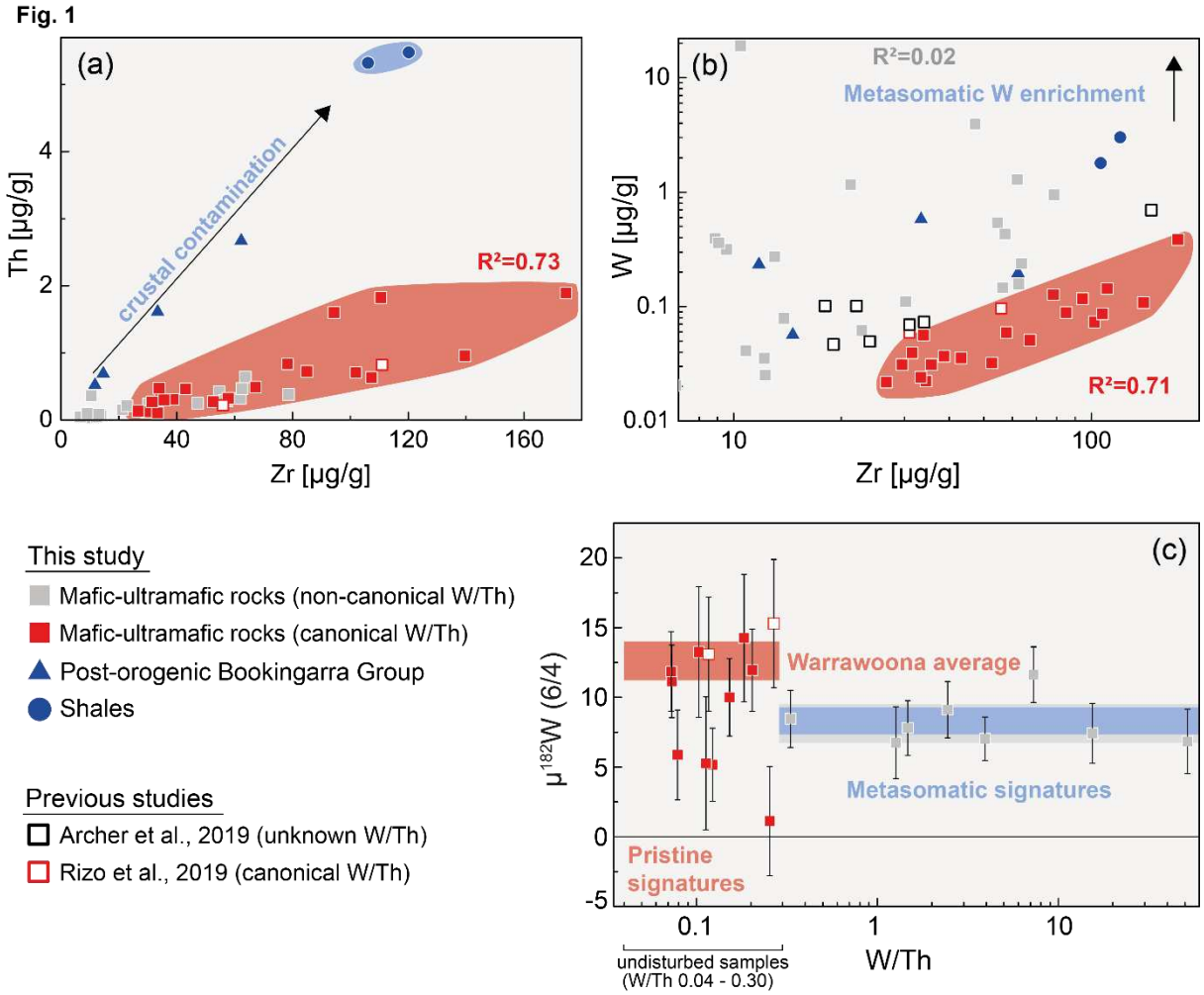

Fig. 2

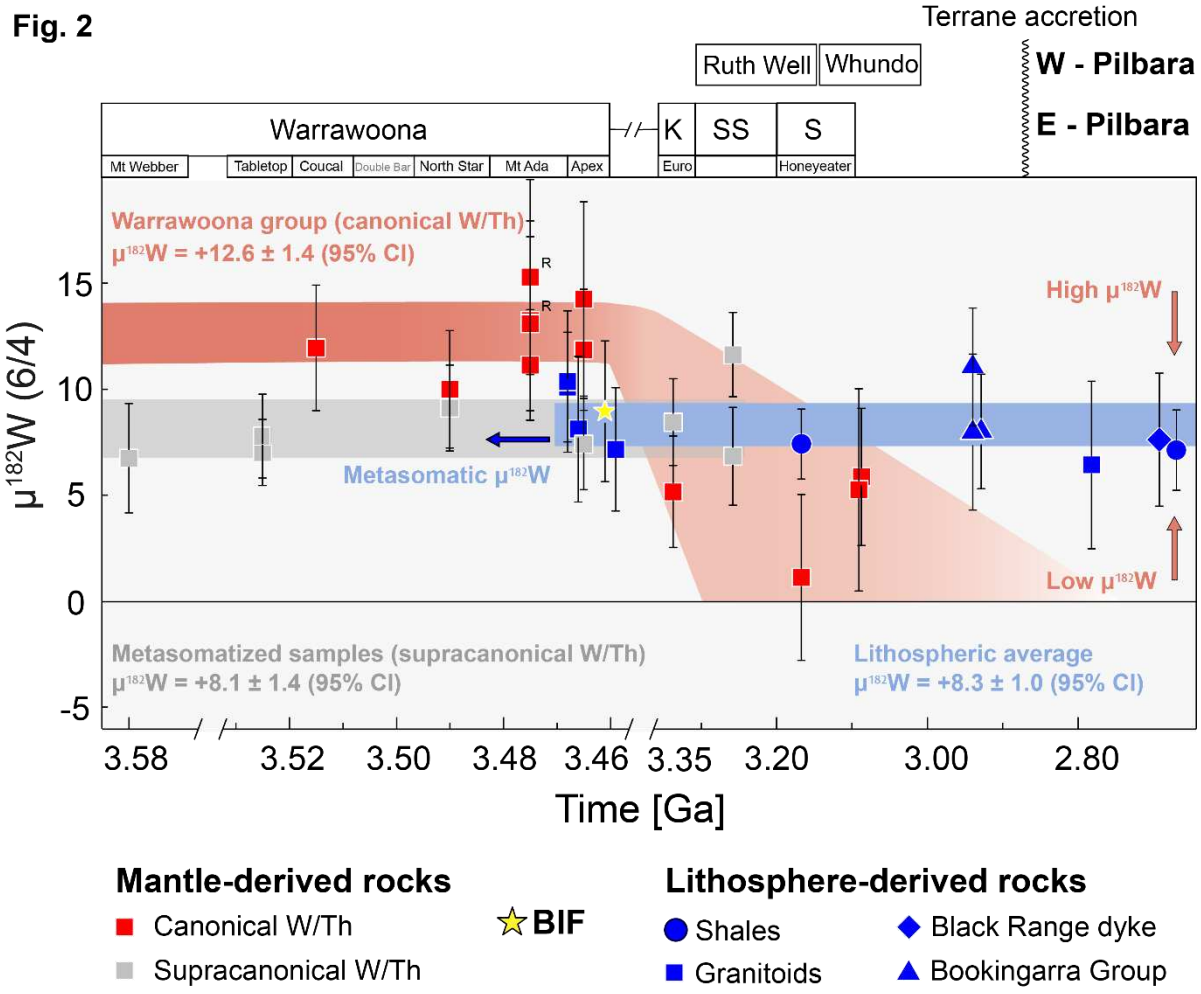
Terrane accretion
Ruth Well
Whundo
W - Pilbara
E - Pilbara
Warrawoona
K
SS
S
Mt Webber
Tabletop
Coucal
Double Bar
North Star
Mt Ada
Apex
Euro
Honeyeater
Warrawoona group (canonical W/Th)
μ182W = +12.6 ± 1.4 (95% CI)
High μ182W
Metasomatic μ182W
Low μ182W
Metasomatized samples (supracanonical W/Th)
μ182W = +8.1 ± 1.4 (95% CI)
Lithospheric average
μ182W = +8.3 ± 1.0 (95% CI)
μ182W (6/4)
15
10
5
0
-5
3.58
3.52
3.50
3.48
3.46
3.35
3.20
3.00
2.80
Time [Ga]
Mantle-derived rocks
Canonical W/Th
Supracanonical W/Th
BIF
Lithosphere-derived rocks
Shales
Granitoids
Black Range dyke
Bookingarra Group

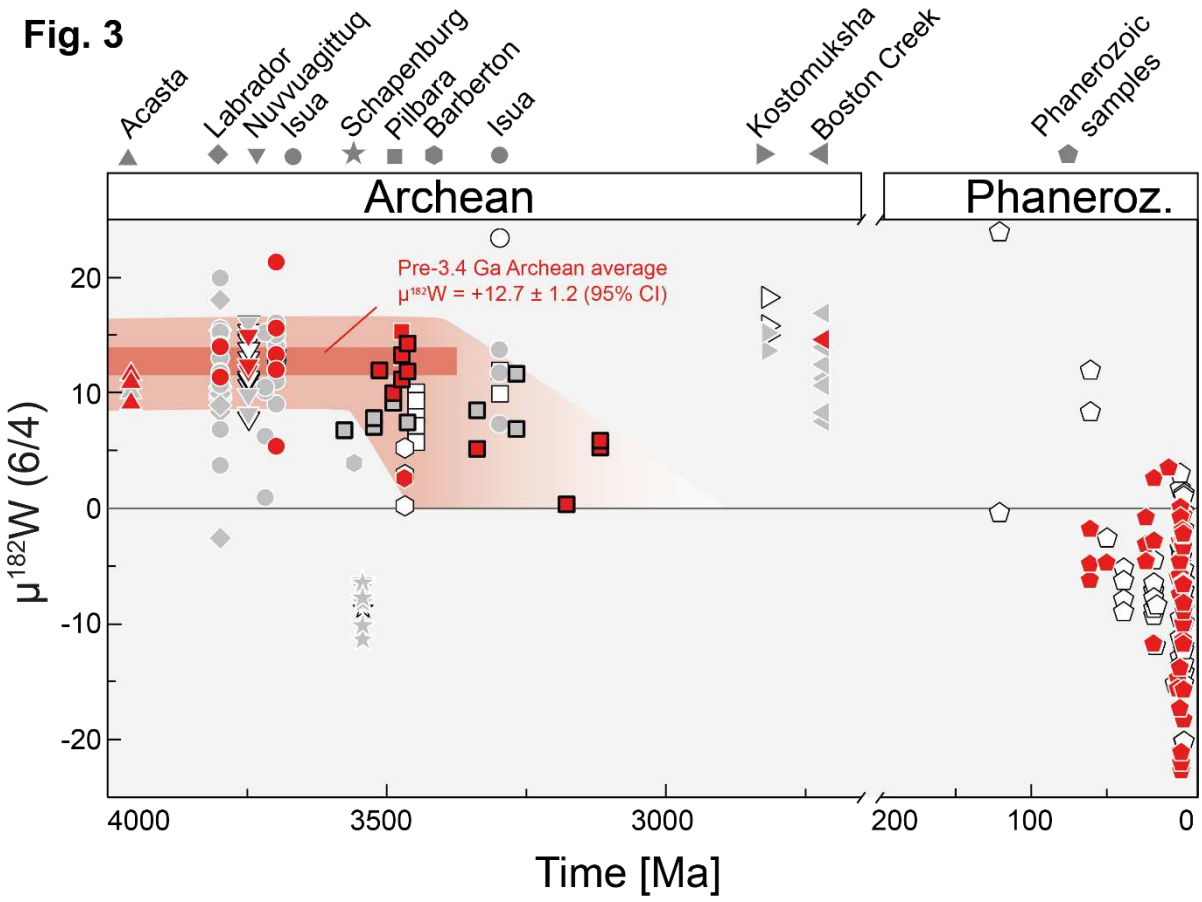

Figure Captions

Fig. 1: **Trace element variation diagrams showing Th and W vs. Zr contents in mafic-ultramafic rocks from the Pilbara Craton (a & b) and high-precision μ^{182}W data for rocks from the Pilbara Craton versus W/Th ratios (c).** All concentration measurements were conducted by isotope dilution. Also included are Pilbara samples that were previously analyzed for their ^{182}W isotope composition(14, 35). **(a)** Nearly all Pilbara samples have preserved robust magmatic differentiation trends for Th vs. Zr, indicating that Th was not significantly affected by secondary processes. Only the post-orogenic samples from the Bookingarra Group were contaminated by crustal components, in line with previous studies(34). **(b)** In contrast to Th, the scattered concentrations of W mirror post-magmatic W enrichment by secondary processes. Primary magmatic differentiation trends are preserved in samples with canonical W/Th ratios. Notably, all samples from ref 26 display strongly elevated W concentrations that indicate post-magmatic W enrichment. **(c)** Samples with undisturbed elemental W budgets (red squares, W/Th lower than 0.30, see SI Appendix) display variable ^{182}W isotope excesses that constitute a progressive diminishing with time (see Fig. 2). Samples with elevated W/Th ratios (grey squares) were affected by secondary W enrichment by metasomatic agents that integrate the ^{182}W isotope composition of the whole Pilbara Craton. Accordingly, these samples display intermediate ^{182}W isotope excesses yielding the same average as lithosphere derived samples (grey and blue bars, respectively).

Fig. 2: High-precision $\mu^{182}W$ analyses for rocks from the Pilbara Craton presented in stratigraphic order. Associated uncertainties refer to the corresponding 95% confidence intervals of multiple digestions (95% CI). Mantle-derived samples with undisturbed elemental W budgets (having canonical W/Th ratios) are represented by red squares, mantle-derived samples that were affected by secondary W-enrichment (supracanonical W/Th ratios) are shown as grey squares. Undisturbed Warrawoona Group samples display an average of $\mu^{182}W$ = +12.6 ± 1.4 ppm (95% confidence interval (CI), n=8, red bar), whereas rocks that were affected by secondary W-enrichment display resolvably lower excesses of ~ +8.1 ± 1.4 ppm (95% CI, n=8; grey bar). Younger mantle derived rocks with undisturbed W budgets display significantly lower ^{182}W excesses. Lithosphere-derived rocks are shown as blue symbols. Granitoid rocks (blue squares) include non-gneissic tonalites and more fractionated and post-orogenic granitoids. Shales (blue circles) provide information about the upper continental crust, whereas lithospheric mafic magmatism is recorded in samples from the Bookingarra and Fortescue groups. The lithospheric samples provide an average $\mu^{182}W$ of +8.3 ± 1.0 ppm (blue bar) which is significantly lower than the average $\mu^{182}W$ of +12.6 ± 1.4 ppm for Warrawoona Group samples with canonical W/Th (red bar). Notably, samples that were affected by secondary W enrichment (grey bar) display the same average as the lithosphere-derived rocks (blue bar). R = previously published data for two samples from the Apex basalt(14), K = Kelly Group, SS = Sulphul Springs Group, S = Soanesville Group

Fig. 3: **Compilation illustrating the secular ^{182}W isotope evolution of the terrestrial mantle**. This dataset includes all available ^{182}W isotope literature data for mantle-derived rocks. For Nuvvuagittuq we assume a minimum emplacement age of 3.75 Ga(50), being well aware that it might be older(51). The literature data are subdivided into samples with overprinted elemental W budgets (grey) and samples with canonical W/Th (red). Symbols with no color fill refer to samples with unknown W/Th ratios. Data for Pilbara rocks presented in this study are squares with thick black frames. References and information on the data compilation are provided in Dataset S4. Error bars are omitted for visual clarity, but uncertainties are given in Dataset S4.

1. S. Labrosse, J. W. Hernlund, N. Coltice, A crystallizing dense magma ocean at the base of the Earth's mantle. *Nature* **450**, 866–869 (2007).

2. M. D. Ballmer, C. Houser, J. W. Hernlund, R. M. Wentzcovitch, K. Hirose, Persistence of strong silica-enriched domains in the Earth's lower mantle. *Nat. Geosci.* **10**, 236–240 (2017).

3. H. Craig, J. E. Lupton, Primordial neon, helium, and hydrogen in oceanic basalts. *Earth Planet. Sci. Lett.* **31**, 369–385 (1976).

4. V. C. Bennett, A. D. Brandon, A. P. Nutman, Coupled 142Nd - 143Nd Isotopic Evidence for Hadean Mantle Dynamics. *Science (80-.).* **318**, 1907–1910 (2007).

5. M. Willbold, T. Elliott, S. Moorbath, The tungsten isotopic composition of the Earth's mantle before the terminal bombardment. *Nature* **477**, 195–198 (2011).

6. T. Kleine, C. Münker, K. Mezger, H. Palme, Rapid accretion and early core formation on asteroids and the terrestrial planets from Hf-W chronometry. *Nature* **418**, 952–955 (2002).

7. T. . Kruijer, T. Kleine, M. Fischer-Gödde, P. Sprung, Lunar tungsten isotopic evidence for the late veneer. *Nature* **520**, 534–537 (2015).

8. M. Touboul, I. S. Puchtel, R. J. Walker, Tungsten isotopic evidence for disproportional late accretion to the Earth and Moon. *Nature* **520**, 530–533 (2015).

9. C.-L. Chou, Fractionation of siderophile elements in the earth´s upper mantle. *Proc. Lunar Planet. Sci. Conf. 9th*, 219–230 (1978).

10. M. Touboul, I. S. Puchtel, R. J. Walker, 182W evidence for long-term preservation of early mantle differentiation products. *Science (80-.).* **335**, 1065–1069 (2012).

11. Rizo, *et al.*, Early Earth Differentiation Investigated Through 142Nd, 182W, and Highly Siderophile Element Abundances in Samples From Isua, Greenland. *Geochim. Cosmochim. Acta* **175**, 319–336 (2016).

12. A. Mundl, *et al.*, Tungsten-182 heterogeneity in modern ocean island basalts. *Nature* **69**, 66–69 (2017).

13. A. Mundl-Petermeier, *et al.*, Anomalous 182W in high 3He/4He ocean island basalts: Fingerprints of Earth's core? *Geochim. Cosmochim. Acta* **271**, 194–211 (2020).

14. H. Rizo, *et al.*, 182W evidence for core-mantle interaction in the source of mantle plumes. *Geochemical Perspect. Lett.* **11**, 6–11 (2019).

15. T. Yoshino, Y. Makino, T. Suzuki, T. Hirata, Grain boundary diffusion of W in lower mantle phase with implications for isotopic heterogeneity in oceanic island basalts by core-mantle interactions. *Earth Planet. Sci. Lett.* **530**, 1–9 (2019).

16. J. R. Reimink, *et al.*, Tungsten Isotope Composition of Archean Crustal Reservoirs and Implications for Terrestrial μ182W Evolution. *Geochemistry, Geophys. Geosystems* **21**, 1–16 (2020).

17. J. Tusch, *et al.*, Uniform 182W isotope compositions in Eoarchean rocks from the Isua region, SW Greenland: the role of early silicate differentiation and missing late veneer. *Geochim. Cosmochim. Acta* **257**, 284–310 (2019).

18. A. Mundl, R. J. Walker, J. R. Reimink, R. L. Rudnick, R. M. Gaschnig, Tungsten-182 in the upper continental crust: Evidence from glacial diamictites. *Chem. Geol.* **494**, 144–152 (2018).

19. J. R. Reimink, T. Chacko, R. A. Stern, L. M. Heaman, The birth of a cratonic nucleus: Lithogeochemical evolution of the 4.02-2.94 Ga Acasta Gneiss Complex. *Precambrian Res.* **281**, 453–472 (2016).

20. J. R. Reimink, *et al.*, No evidence for Hadean continental crust within Earth's oldest evolved rock unit. *Nat. Geosci.* **9**, 777–780 (2016).

21. M. R. Mohan, B. S. Kamber, S. J. Piercey, Boron and arsenic in highly evolved Archean felsic rocks: Implications for Archean subduction processes. *Earth Planet. Sci. Lett.* **274**, 479–488 (2008).

22. S. Klemme, S. Prowatke, K. Hametner, D. Günther, Partitioning of trace elements between rutile and silicate melts: Implications for subduction zones. *Geochim. Cosmochim. Acta* **69**, 2361–2371 (2005).

23. J. R. Reimink, *et al.*, Petrogenesis and tectonics of the Acasta Gneiss Complex derived from integrated petrology and142Nd and182W extinct nuclide-geochemistry. *Earth Planet. Sci. Lett.* **494**, 12–22 (2018).

24. J. Liu, M. Touboul, A. Ishikawa, R. J. Walker, D. Graham Pearson, Widespread tungsten isotope anomalies and W mobility in crustal and mantle rocks of the Eoarchean Saglek Block, northern Labrador, Canada: Implications for early Earth processes and W recycling. *Earth Planet. Sci. Lett.* **448**, 13–23 (2016).

25. M. Touboul, J. Liu, J. O'Neil, I. S. Puchtel, R. J. Walker, New insights into the Hadean mantle revealed by 182W and highly siderophile element abundances of supracrustal rocks from the Nuvvuagittuq Greenstone Belt, Quebec, Canada. *Chem. Geol.* **383**, 63–75 (2014).

26. M. J. Van Kranendonk, R. Hugh Smithies, A. H. Hickman, D. C. Champion, Review: Secular tectonic evolution of Archean continental crust: interplay between horizontal and vertical processes in the formation of the Pilbara Craton, Australia. *Terra Nov.* **19**, 1–38 (2007).

27. R. H. Smithies, M. J. Van Kranendonk, D. C. Champion, It started with a plume - Early Archaean basaltic proto-continental crust. *Earth Planet. Sci. Lett.* **238**, 284–297 (2005).

28. E. Hasenstab, *et al.*, Evolution of the early to late Archean mantle from Hf-Nd-Ce isotope systematics in basalts and komatiites from the Pilbara Craton. *Earth Planet. Sci. Lett.* (2020), https://doi.org./10.1016/j.epsl.2020.116627.

29. Smithies, D. C. Champion, M. J. Van Kranendonk, H. M. Howard, A. H. Hickman, Modern-style subduction processes in the Mesoarchaean: Geochemical evidence from the 3.12 Ga Whundo intra-oceanic arc. *Earth Planet. Sci. Lett.* **231**, 221–237 (2005).

30. M. J. Van Kranendonk, R. Hugh Smithies, A. H. Hickman, M. T. D. Wingate, S. Bodorkos, Evidence for Mesoarchean (~3.2 Ga) rifting of the Pilbara Craton: The missing link in an early Precambrian Wilson cycle. *Precambrian Res.* **177**, 145–161 (2010).

31. W. D. Maier, *et al.*, Progressive mixing of meteoritic veneer into the early Earth's deep mantle. *Nature* **460**, 620–623 (2009).

32. J. Völkening, M. Köppe, K. G. Heumann, Tungsten isotope ratio determinations by negative thermal ionization mass spectrometry. *Int. J. Mass Spectrom. Ion Process.* **107**, 361–368 (1991).

33. S. König, *et al.*, The Earth's tungsten budget during mantle melting and crust formation. *Geochim. Cosmochim. Acta* **75**, 2119–2136 (2011).

34. R. H. Smithies, D. C. Champion, S. S. Sun, Evidence for early LREE-enriched mantle source regions: Diverse magmas from the c. 3·0 Ga Mallina Basin, Pilbara Craton, NW Australia. *J. Petrol.* **45**, 1515–1537 (2004).

35. G. J. Archer, *et al.*, Lack of late-accreted material as the origin of 182 W excesses in the Archean mantle : Evidence from the Pilbara Craton , Western Australia. *Earth Planet. Sci. Lett.* **528**, 115841 (2019).

36. W. D. Maier, *et al.*, Progressive mixing of meteoritic veneer into the early Earths deep mantle. *Nature* **460**, 620–623 (2009).

37. V. Debaille, *et al.*, Stagnant-lid tectonics in early Earth revealed by 142Nd variations in late Archean rocks. *Earth Planet. Sci. Lett.* **373**, 83–92 (2013).

38. J. H. Bédard, Stagnant lids and mantle overturns: Implications for Archaean tectonics, magmagenesis, crustal growth, mantle evolution, and the start of plate tectonics. *Geosci. Front.* **9**, 19–49 (2018).

39. Q.-F. Mei, J.-H. Yang, Y.-F. Wang, H. Wang, P. Peng, Tungsten isotopic constraints on homogenization of the Archean silicate Earth: Implications for the transition of tectonic regimes. *Geochim. Cosmochim. Acta* (2019) https:/doi.org/10.1016/j.gca.2019.07.050.

40. E. A. Belousova, *et al.*, The growth of the continental crust: Constraints from zircon Hf-isotope data. *Lithos* **119**, 457–466 (2010).

41. J. A. Pearce, Geochemical fingerprinting of oceanic basalts with applications to ophiolite classification and the search for Archean oceanic crust. **100**, 14–48 (2008).

42. S. B. Shirey, S. H. Richardson, Start of the wilson cycle at 3 Ga shown by diamonds from subcontinental mantle. *Science (80-.).* **333**, 434–436 (2011).

43. B. Dhuime, A. Wuestefeld, C. J. Hawkesworth, Emergence of modern continental crust about 3 billion years ago. *Nat. Geosci.* **8**, 552–555 (2015).

44. C. O'Neill, A. Lenardic, L. Moresi, T. H. Torsvik, C. T. A. Lee, Episodic Precambrian subduction. *Earth Planet. Sci. Lett.* **262**, 552–562 (2007).

45. T. Gerya, Geodynamics of the early Earth: Quest for the missing paradigm. *Geology* **47**, 1006–1007 (2019).

46. I. S. Puchtel, J. Blichert-Toft, M. Touboul, R. J. Walker, 182W and HSE constraints from 2.7 Ga komatiites on the heterogeneous nature of the Archean mantle. *Geochim. Cosmochim. Acta* **228**, 1–26 (2018).

47. Q.-F. Mei, J.-H. Yang, Y.-F. Wang, H. Wang, P. Peng, Tungsten isotopic constraints on homogenization of the Archean silicate Earth: Implications for the transition of tectonic regimes. *Geochim. Cosmochim. Acta* **278**, 51–64 (2020).

48. C. O'Neill, V. Debaille, The evolution of Hadean-Eoarchaean geodynamics. *Earth Planet. Sci. Lett.* **406**, 49–58 (2014).

49. M. B. Weller, A. Lenardic, Hysteresis in mantle convection: Plate tectonics systems. *Geophys. Res. Lett.* **39**, 3–7 (2012).

50. N. L. Cates, S. J. Mojzsis, Pre-3750 Ma supracrustal rocks from the Nuvvuagittuq supracrustal belt, northern Québec. *Earth Planet. Sci. Lett.* **255**, 9–21 (2007).

51. J. O´Neil, R. W. Carlson, D. Francis, R. K. Stevenson, Neodymium-142 Evidence for Hadean Mafic Crust. *Science (80-.).* **321**, 1828–1832 (2008).

Supplementary Information Text

Analytical protocol

Concentration measurements for high-field-strength elements (HFSE), W, U, and Th were conducted by isotope dilution, using mixed isotope tracers that are enriched in ^{229}Th-^{233}U-^{236}U and ^{183}W-^{180}Ta-^{94}Zr, respectively. Around 120 mg of sample powder were spiked and digested using a previously described protocol(17). After sample-spike equilibration, we separated our sample solution (30% aliquot for U, Th, and W analyses and 70% for HFSE analyses). The chemical separation for HFSE followed a previously published protocol(52). The 30% aliquot for U, Th and W analyses was loaded onto BioRad Poly-Prep® columns filled with 1.6ml Eichrom TRU-Spec® resin (200-400 mesh) atop 0.4ml Eichrom prefilter® material. Tungsten and most matrix components of the 30% aliquot were eluted during loading (1.5N HNO_3) and subsequent rinsing (2 x 5/8 resin volumes (rv) of 1.5 M HNO_3). The subsequent separation of U and Th on TRU-Spec® resin followed a previously published protocol(53). In previous protocols(17, 52), U and Th were first separated during an HFSE protocol in 2 M HF prior to loading onto TRU-Spec® resin. By first loading our 30% aliquot onto TRU-Spec® resin, we avoid the formation of insoluble Th bearing fluorides. Tungsten was subsequently separated from residual matrix components using BioRad Poly-Prep® columns filled with 2ml AG-1-X8 resin(54). Tungsten concentration measurements for granites were performed differently, using a ^{180}W-^{183}W double-spike technique(55). All high-precision isotope dilution analyses were performed on a Thermo Fisher® Neptune Plus Multicollector ICP-MS at Cologne(52, 54, 56). For measurements of other trace elements we used the analytical protocol described by Tusch et al.(17). Trace element concentrations were measured using a quadrupole ICP-MS at the Institut für Geowissenschaften at CAU Kiel(57).

The chemical purification of W for high-precision isotope composition analyses follows a previously published analytical protocol(17) that was only slightly modified to be able to process up to 1.6 g rock powder per column. The final W bearing cut after the third stage column (Eichrom™ TEVA resin) was directly loaded onto TODGA resin (1ml TODGA resin in Spectra/Chrom® 45µm PP MiniColumns) that purifies W more efficiently from remaining matrix elements and Ti(58). During loading in 5 M HCl and subsequent rinsing with 2 x 6.5 rv 3 M HNO_3 the remaining Ti and most other remaining matrix elements pass through the resin. By subsequently rinsing with 3 x 6.5 rv 8 M HNO_3 residual Ca is also eluted. During these washing steps W is completely retained on the column and can be finally eluted in 3 x 5 rv 0.56 M HNO_3 – 0.24 M HF. Remaining impurities in our final W cut after processing 1.6 g rock powder (felsic matrix) were 5 ng/ml Na, 11 ng/ml Mg, 4 ng/ml Al, 2 ng/ml K, 21 ng/ml Ca, 0.1 ng/ml Ti, 1.2 ng/ml Ta, 2 ng/ml Nb and 0.5 ng/ml Mo. Considering the initial weight of sample material (1.6 g) this translates to fractions in the ppt range.
The setup for high-precision ^{182}W isotope measurements has also been described in detail in a previous study(17). In short, the analyses of the Pilbara samples were run over a period of 22 months (February 2018 – November 2019) at an average signal sensitivity of 4.5 V on ^{182}W (using 10^{11} Ohm amplifiers) for a ~50 ng/ml W sample solution at an uptake rate of ca. 60 µl/min. The measurements of sample solutions were run at intensities between 2.0 and 27.5 V on ^{182}W, corresponding to 23 – 274 ng/ml solutions. Samples were always bracketed by a concentration-matched certified reference material (NIST SRM 3163) to report relative ^{182}W isotope compositions. For all samples we performed multiple measurements (n = 9-23) to obtain a statistically significant population, and uncertainties for average W isotope composition values are correspondingly reported as 95% confidence intervals (95% CI). Average values and associated 95% CI are reported in Dataset S1, while corresponding single measurements with their internal run statistics (2 s.e.) are given in Dataset S2. For ^{182}W the 95% CI for repeatedly measured samples (n = 9-23) ranged between ±1.6 ppm and ± 4.8 ppm (average of ±3.0 ppm). Differences in the 95% CI mainly result from differences in beam intensities.
Previous studies reported massive nuclear field shift (NFS) effects on the odd isotope ^{183}W during measurements with a MC-ICP-MS(35, 59, 60). This mass-independent fractionation can create analytical artifacts when internal normalizations employ mass 183 to correct for instrumental mass bias (e.g. ^{186}W/^{183}W, denoted ´6/3´)(59). Contrary to previous studies (35, 59, 60), our analytical protocol(17) ensures that NFS effects on μ^{182}W are minor and within the analytical uncertainty (for μ^{182}W (6/3) on average ± 3.0ppm). For most measurements (93%), the normalization to 6/3 or to 6/4 (^{186}W/^{184}W), respectively, caused no resolvable difference in mass bias corrected μ^{182}W values. However, to avoid even small NFS effects we prefer the normalization to ^{186}W/^{184}W for instrumental mass bias corrections.

Our long-term reproducibility is inferred from repeated measurements of two in-house rock reference materials (historical La Palma basalt "*LP1*" and a 3455 Ma gneiss from Swaziland, labeled "*AGC 351*"(61)). Along with our samples, the in-house rock standards were always passed individually through

our separation protocol and measured in every session at different run-conditions (variable procedural yields at different signal intensities). In total, we performed 16 measurements for sample LP1 (235 single measurements) and 11 measurements for sample AGC 351 (151 single measurements). The session averages for $\mu^{182}W$ of both samples overlap within their 95% CI (LP1 = -1.3 ± 1.1 ppm and AGC 351 = -0.1 ± 1.2 ppm) and are indistinguishable from the NIST reference material (Supplementary Fig. S2) and previously reported long-term averages for the same sample powders(17). The reproducibility of both in-house rock reference materials relative to NIST SRM 3163 is given by the 2 SD of the corresponding average $\mu^{182}W$ (-1.3 ± 4.3 ppm for LP1 and -0.1 ± 3.5 ppm for AGC 351). The somewhat poorer reproducibility of sample LP 1 stems from lower signal intensities (2.1 – 15.0 volts on ^{182}W) when compared to sample AGC 351 (8.2 – 27.5 volts on ^{182}W).
Our average procedural yields were 77% (70% of samples above 70%, 24% between 60% and 70%) with only three samples below 60% (7% of all samples). Total procedural W blanks were measured on a Thermo Fisher® Neptune Plus Multicollector ICP-MS at the University of Cologne after adding a ^{180}W-^{183}W double-spike tracer(55). Blanks were typically below 500 pg (137-471 pg) which corresponds to less than 1 % blank contribution. Three erratic blank values were higher (1401, 1804 and 3427 pg) but only contributed up to 4.5 % to the total analyte. Considering the average excess for undisturbed samples from the Warrawoona Group ($\mu^{182}W$ = +12.6 ± 1.4 ppm) and our average uncertainty on the sample averages (± 3.0 ppm) a blank contribution of 4.5% carrying modern upper mantle like ^{182}W isotope composition ($\mu^{182}W$ = 0) would propagate into our $\mu^{182}W$ values to less than 1ppm.

Geological background

The Pilbara Craton of Western Australia has been subdivided into the East Pilbara Terrane (EPT), West Pilbara Superterrane (WPS, comprised of three separate terranes), and the Kuranna Terrane(26). Rocks from the EPT and WPS display dissimilar geochemical, geochronological, and structural characteristics, reflecting markedly different processes of crust formation(62). The 3.52-3.18 Ga East Pilbara Terrane is the ancient nucleus of the craton and a global type example for the dome-and-keel geometry that is unique to many Archean terranes(63). Granitoid domes are ovoid, multi-component intrusive complexes that are separated by narrow, mostly steeply dipping cuspate greenstone belts, and encircled by ring faults(64). EPT greenstones comprise 3.52 – 3.18 Ga old, predominantly tholeiitic and lesser komatiitic volcanic rocks, with minor interbedded sediments, of the Pilbara Supergroup that is subdivided into four unconformity-bound groups (Warrawoona, Kelly, Sulphur Springs and Soanesville). The oldest three volcanic groups were derived from moderately depleted mantle sources(27, 28) and emplaced during distinct mantle plume events(65) similar to modern plateau basalts(26, 66). The Honeyeater Basalt of the youngest Soanesville Group is interpreted as the product of plume-initiated rifting that caused intra-continental extension and magmatism at the start of a Wilson cycle(30).

A rifted fragment of the EPT is inferred in the WPS (Karratha Terrane) that, together with MORB-like rocks of the Regal Terrane, and subduction-related rocks of the Sholl Terrane, accreted to form the WPS at c. 3.07 Ga(26, 29). The Sholl Terrane comprises the 3.13-3.11 Ga Whundo Group, a sequence with geochemical characteristics that are consistent with their derivation from a depleted mantle source that was variably affected by metasomatic enrichment in an arc-like setting(29).

The Pilbara Supergroup of the EPT erupted on a > 3.53 Ga proto-continental basement that was most likely a heterogeneous mix of mafic and felsic lavas and TTGs (tonalites, trondhjemites and granodiorites) with a common tholeiitic parental magmatic source(67). Multiple lines of evidence for the presence of an older basement(64) include the presence of older gabbroic-anorthositic enclaves (Mount Webber Gabbro) embedded in granitic rocks of the Shaw Granitic Complex(68, 69), older TTG enclaves, and abundant inherited zircons(64). The burial of heat-producing ancient TTGs into the middle crust, together with conductive and convective heat brought by excessive mantle melting events, caused re-melting of early TTGs, which resulted in thermal softening of the middle crust(70). This lead to diapirism of granitoid melts ascending from the middle crust, and to the sinking of the dense volcanic rocks from the greenstone successions during partial convective overturn, which lead to the observed dome-and-keel geometry(63).

Granitic rocks of the EPT have been divided into five supersuites that were emplaced during discrete intervals between 3.49 and 3.22 Ga(26) (3.49-3.46 Ga Callina, 3.45-3.42 Tambina, 3.33-3.29 Emu Pool, 3.27-3.22 Ga Cleland supersuites). The large-scale granitoid domes are polyphase complexes that initially derived through melting from a mafic (tholeiitic) protocrust and earlier TTG rocks(67, 71) and subsequently evolved to more evolved high-K granitic compositions (predominantly monzogranites)

through successive melting events. Younger granitic phases were emplaced into the cores of the developing domes(72) during partial convective overturn.

After c. 3.07 Ga, when accretion of the WPS onto the EPT took place, volcanic and sedimentary rocks of the De Grey Supergroup were deposited from 3.02 Ga in several basins that formed in response to lithospheric extension(26). Mafic volcanic rocks of the Bookingarra Group and associated intrusive rocks were emplaced between ~3.0 and 2.95 Ga. The Bookingarra Group unconformably overlies volcano-sedimentary rocks of the Whim Creek and Croydon Groups at the western end of the late-tectonic Mallina Basin. These older rocks derived from a metasomatized, lithospheric mantle source that was refertilized by subducted sediments during the formation of the Whundo Group in a subduction zone-like setting ca. 150 Ma earlier(34). The tectono-magmatic history of the Pilbara Craton was completed by the emplacement of ca. 2.85 Ga post-tectonic granites of the Split Rock Supersuite(26). Emplacement of ca. 2.78 Ga(73) lithosphere-derived rift-related dikes of the Black Range Dolerite Suite record the onset of rifting and deposition of the unconformably overlying Fortescue Group.

Sample selection

Most mantle-derived samples from the EPT were collected in the Marble Bar greenstone belt and in the North Pole Dome area (Panorama greenstone belt) where rocks were only affected by low grade metamorphism and low strain(26). Samples from the oldest Coonterunah Subgroup of the Warrawoona Group were collected in the East Strelley greenstone belt and samples from the Honeyeater Basalt from the Soanesville greenstone belt (Supplementary Fig. S1). The low metamorphic grade is most promising for preservation of primary elemental W budgets.

To expand our dataset for mantle-derived rocks from the EPT we also sampled a recently described 3.59 Ga magmatic suite (Mount Webber Gabbro, Pil17-07) that was shown to predate the oldest rocks from the Warrawoona Group and that are thought to represent remnants of an early proto-crust(68, 69). Our sample was collected in an outcrop on the eastern bank of the Shaw River where anorthositic host rocks within the tonalites contain gabbroic enclaves(68).

Mantle-derived rocks from the WPS comprise samples from the Sholl Terrane (Whundo Group, Pil16-67, -74, -75) and Karratha Terrane (Ruth Well Formation, Pil16-66b). Our samples from the Whundo Group were collected in the same outcrop area as previously described in detail by pioneering studies on the Whundo Group(29).

Granitoid samples from the multi-phase dome complexes of the EPT include those from the low-strain North Shaw Suite (3.49-3.46 Ga Callina Supersuite) in the northern part of the Shaw Granitic Complex, which comprises exceptionally well preserved tonalites that still display igneous textures(74). We sampled two undeformed to weakly-foliated tonalites from the North Shaw Suite (Pil16-34 & -35), as well as younger (Pil16-36a) and more fractionated gneissic TTGs (Pil16-12, -36a, -41) to cover a suite of rocks that represent lithostratigraphic and petrological end-members of the long-lived granitic complexes. Additionally, we sampled lithosphere-derived mafic rocks from the Bookingarra (Pil16-63, -65 & -75) and Fortescue Group (Black Range dolerite, Pil16-31) to better constrain the ^{182}W isotope composition of the subcontinental lithosphere within the Pilbara Craton.

Secular evolution of ^{182}W isotope anomalies

To better understand the secular evolution of ^{182}W isotope anomalies in Earth´s mantle, we compiled all literature data for ^{182}W isotope compositions measured in mantle-derived rocks. We note, that we excluded samples from the Ameralik dike suite (SW Greenland), because they tap multiple unknown source reservoirs that were likely overprinted by crustal-like material (75, 76). Supplementary Dataset S4 provides an overview and lists all references for ^{182}W data, elemental concentrations of W and Th, and, if available, ^{142}Nd data. In total, 22 studies reported 220 ^{182}W isotope compositions for mantle-derived rocks, with 117 samples from the Archean, only 1 sample from the Proterozoic(77) and 102 samples of Phanerozoic age. It becomes apparent that most studies have only provided snapshots within the ^{182}W isotope evolution of individual Archean cratons(10, 24, 25, 46, 78). We further screened this compilation for samples that were not substantially affected by secondary W-enrichment. Indeed, 96% of the Phanerozoic samples in our compilation that report elemental concentrations for W and Th (n=50) display canonical W/Th ratios. Only two samples have slightly supracanonical W/Th ratios of 0.26 and 0.27, respectively. The Phanerozoic samples with canonical W/Th ratios are characterized by

an average deficit in μ^{182} of -6.4 ± 1.7 ppm (95% CI) and display an average W/Th of 0.144, which perfectly overlaps with the combined average for fresh MORB and OIB samples (W/Th = 0.150)(33). We consider samples as being significantly disturbed in their elemental W budged, where W/Th ratios are more than twice as high as the average canonical W/Th ratio (i.e. W/Th above 0.30). By this restriction, only 18 out of 117 Archean samples, which were analyzed for their ^{182}W isotope composition (15%), have preserved a W budget that is primary and reflects an unmodified mantle source. It has been argued that elevated W/Th ratios in mantle-derived rocks from the Archean might be a non-uniformitarian Archean feature(79). However, as demonstrated in this study the Archean suite analyzed here comprises many rocks with primary W budgets as present day MORB and OIB.

After screening the global dataset, it becomes apparent, that Archean rocks with canonical W/Th ratios display uniform excesses before ~3.4 Ga of ca. 13 ppm. Exceptions are two ~ 3.7 Ga old amphibolites from Isua (sample 00-044: μ^{182}W = +21.3 ± 5.3 ppm; sample 00-008: μ^{182}W = +5.4 ± 7.2 ppm)(11). We regard these two samples as outliers for two reasons. First, it was not possible to reproduce results for ^{182}W isotope compositions on the same powder splits for other rocks that displayed markedly different ^{182}W isotope compositions than typically observed for Isua rocks (samples S31 & S33)(17). Second, other ~ 3.7-3.8 Ga old amphibolites and metabasalts from Isua with canonical W/Th ratios display homogeneous excesses of ca. +13 ppm(5, 17, 80). As demonstrated by our study on rocks from the Pilbara Craton, the ^{182}W isotope composition of mantle-derived rocks with supracanonical W/Th ratios are dominated by metasomatic agents that re-mix reservoirs of variable ^{182}W isotope compositions. If not taken into consideration, this can lead to ambiguous models on the origin of early formed mantle heterogeneities and on the time-scales of mantle convection. Moreover, overprinted elemental W budgets caused a decoupling of ^{182}W isotope and HSE systematics, thereby also biasing conclusions on the late-accretion history of the Earth(10, 35).

Fig. S1

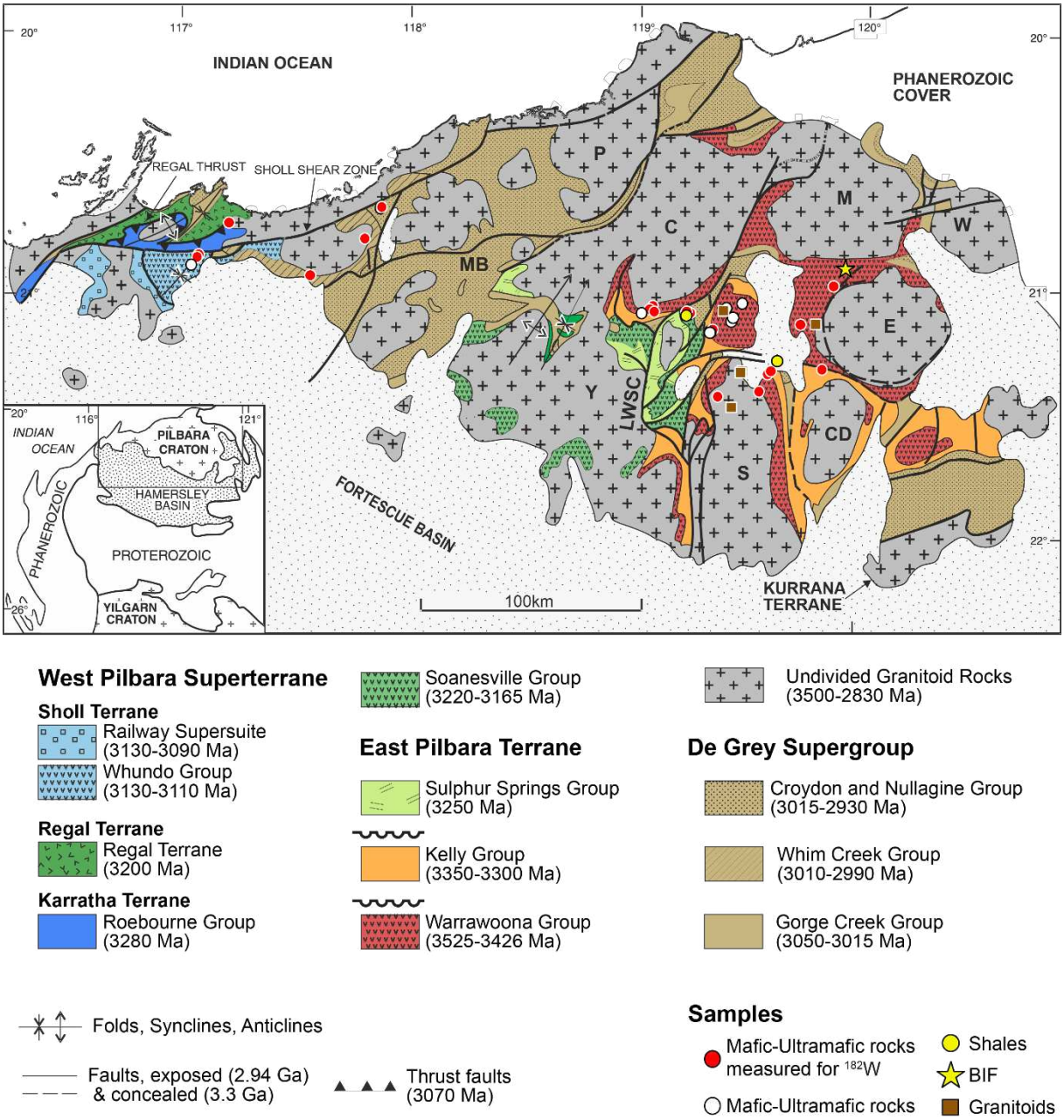

Fig. S1: **Simplified geological map of the Pilbara Craton, NW Australia showing the sample localities covered in this study**. The map is modified from previous studies(26, 30). Shown are the main groups of the West Pilbara Superterrane and East Pilbara Terrane. Both terranes are unconformably overlain by sedimentary rocks of the De Grey Supergroup. LWSZ = Lalla Rookh-Western Shaw structural corridor; MB = Mallina Basin. The older greenstones are intruded by diverse granitoid complexes: M = Muccan; W = Warrawagine; E = Mount Edgar; CD = Corunna Downs; S = Shaw; Y = Yule; C = Carlindie; P = Pippingarra.

Fig. S2

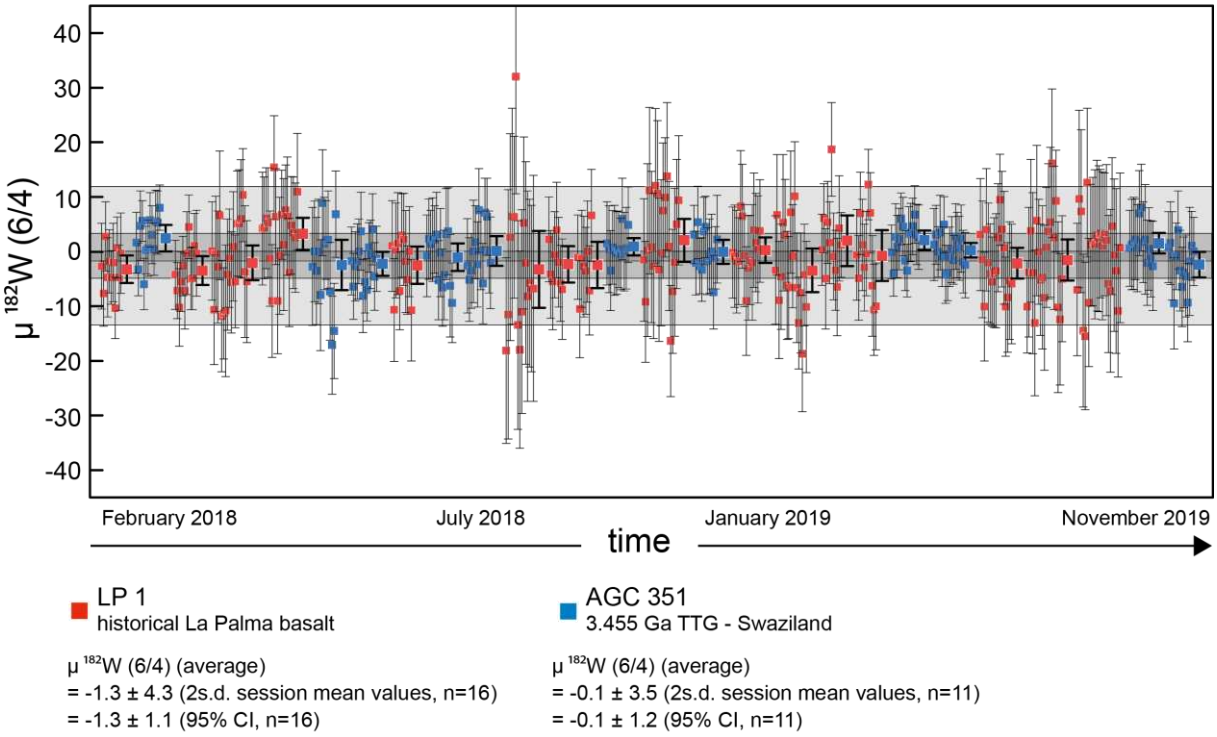

Fig. S2: Long-term reproducibility for $\mu^{182}W$ (6/4), inferred from the repeated analysis of multiple digestions for our in-house reference materials AGC 351 and LP1 reported relative to W NIST SRM 3136. Small symbols refer to single measurements and larger symbols give the average for the corresponding analytical session. For the single measurements, error bars refer to the internal run statistic (2 SE). The uncertainty for the session mean values are given by the corresponding 95% CI. The long-term reproducibility for our two in-house reference materials with variable composition (mafic LP1 and felsic AGC 351) are given by the 2 SD of the session mean values. The poorer reproducibility and larger scatter of sample LP 1 stems from lower signal intensities when compared to sample AGC 351.

Dataset S1: Tungsten isotope composition of Pilbara samples and in-house rock reference materials. Values for $\mu^{182}W_{corr}$ were corrected for the nuclear field shift (NFS) effect on ^{183}W, when normalized to $^{186}W/^{183}W$ (6/3), using the measured $\mu^{184}W$ (6/3) and $\mu^{182}W$ (6/3) values and the relation $\mu^{182}W\ (6/3)_{corr} = \mu^{182}W\ (6/3)_{measured} - (1.962 \times \mu^{184}W\ (6/3))$(81). Notably, our analytical protocol(17) ensures that in most of the cases (93%), NFS effects for $\mu^{182}W$ in our study were within the range of the analytical uncertainty (for $\mu^{182}W$ (6/3) on average ± 3.0ppm) as opposed to previous studies that reported massive NFS effects during ^{182}W isotope measurements with MC-ICP-MS(35, 59, 60).

Dataset S2: Results for single W isotope measurements of Pilbara samples and in-house rock reference materials. Single measurements for individual digestions (characterized by small letters) agree within uncertainty (int. 2SE) and are therefore pooled and reported as averages with corresponding 95% confidence limits. In some cases, leftover solutions from individually measured digestions were combined to increase the number of repeated measurements. In four cases (160245, 179738, Pil 16-51, Pil 16-24) individual digestions were combined from the beginning.

Dataset S3: Major, minor and trace element data as well as GPS coordinates of sample localities for rock samples from the Pilbara Craton. Data in bold and italic (Zr, Nb, Ta, W, Th, and U) were determined by isotope dilution. n.d. = not determined

Dataset S4: Compilation of all available ^{182}W isotope literature data available for mantle-derived rocks. Also given are elemental concentrations for W and Th. References for ^{182}W and ^{142}Nd isotope compositions, as well as for elemental W and Th concentrations are indicated by small letters and also reported. For every location, samples with undisturbed W concentrations are given first (by bold characters), followed by samples with overprinted elemental W budgets and samples where Th concentrations were not reported.

SI References

52. M. M. Thiemens, P. Sprung, R. O. C. Fonseca, F. P. Leitzke, C. Münker, Early Moon formation inferred from hafnium–tungsten systematics. *Nat. Geosci.* **12** (2019).

53. X. Luo, M. Rehkämper, D.-C. Lee, A. N. Halliday, High precision 230Th/232Th and 234U/238U measurements using energyfiltered ICP magnetic sector multiple collector mass spectrometry. *Int. J. Mass Spectrom. Ion Process.* **171**, 105–117 (1997).

54. T. Kleine, K. Mezger, C. Münker, H. Palme, a. Bischoff, 182Hf-182W isotope systematics of chondrites, eucrites, and martian meteorites: Chronology of core formation and early mantle differentiation in Vesta and Mars. *Geochim. Cosmochim. Acta* **68**, 2935–2946 (2004).

55. F. Kurzweil, C. Münker, J. Tusch, R. Schoenberg, Accurate stable tungsten isotope measurements of natural samples using a 180 W- 183 W double-spike. *Chem. Geol.* **476**, 407–417 (2017).

56. S. Weyer, C. Münker, M. Rehkämper, K. Mezger, Determination of ultra-low Nb, Ta, Zr and Hf concentrations and the chondritic Zr/Hf and Nb/Ta ratios by isotope dilution analyses with multiple collector ICP-MS. *Chem. Geol.* **187**, 295–313 (2002).

57. C.-D. Garbe-Schönberg, Simultaneous Determination of Thirty-Seven Trace Elements in Twenty-Eight International Rock Standards By Icp-Ms. *Geostand. Newsl.* **17**, 81–97 (1993).

58. A. Pourmand, N. Dauphas, Distribution coefficients of 60 elements on TODGA resin: Application to Ca, Lu, Hf, U and Th isotope geochemistry. *Talanta* **81**, 741–753 (2010).

59. T. S. Kruijer, T. Kleine, No 182 W excess in the Ontong Java Plateau source. *Chem. Geol.* **485**, 24–31 (2018).

60. S. Tappe, G. Budde, A. Stracke, A. Wilson, T. Kleine, The tungsten-182 record of kimberlites above the African superplume: Exploring links to the core-mantle boundary. *Earth Planet. Sci. Lett.* **547**, 116473 (2020).

61. A. Kröner, *et al.*, Generation of early Archaean grey gneisses through melting of older crust in the eastern Kaapvaal craton, southern Africa. *Precambrian Res.* **255**, 823–846 (2014).

62. R. H. Smithies, *et al.*, Two distinct origins for Archean greenstone belts. *Earth Planet. Sci. Lett.* **487**, 106–116 (2018).

63. M. J. Van Kranendonk, W. J. Collins, A. Hickman, M. J. Pawley, Critical tests of vertical vs. horizontal tectonic models for the Archaean East Pilbara Granite-Greenstone Terrane, Pilbara Craton, Western Australia. *Precambrian Res.* **131**, 173–211 (2004).

64. M. J. Van Kranendonk, A. H. Hickman, R. H. Smithes, D. R. Nelson, Geology and tectonic evolution of the Archean North Pilbara Terrain, Pilbara Craton, Western Australia. *Econ. Geol.* **97**, 695–732 (2002).

65. N. R. Arndt, G. Bruzak, T. Reischmann, The oldest continental and oceanic plateaus: geochemistry of basalts and komatiites of the Pilbara craton, Australia. *Geol. Soc-. Am.* **352**, 359–387 (2001).

66. K. C. Condie, High field strength element ratios in Archean basalts: A window to evolving sources of mantle plumes? *Lithos* **79**, 491–504 (2005).

67. R. H. Smithies, D. C. Champion, M. J. Van Kranendonk, "The oldest well-preserved felsic volcanic rocks on Earh: Geochemical clues to the early evolution of the Pilbara Supergroup and Implications for the growth of a Paleoarchean protocontinent" in *Earth´s Oldest Rocks*, Second Edi, (2019), pp. 463–486.

68. N. J. McNaughton, M. D. Green, W. Compston, I. S. Williams, Are anorthositic rocks basement to the Pilbara Craton? *Geol. Soc. Aust.* **Abstracts**, 272–273 (1988).

69. A. Petersson, *et al.*, A new 3 . 59 Ga magmatic suite and a chondritic source to the east Pilbara Craton. *Chem. Geol.* **511**, 51–70 (2019).

70. M. Sandiford, M. J. Van Kranendonk, S. Bodorkos, Conductive incubation and the origin of dome-and-keel structure in Archean granite-greenstone terrains: A model based on the eastern Pilbara Craton, Western Australia. *Tectonics* **23**, 1–19 (2004).

71. M. J. Bickle, *et al.*, Origin of the 3500-3300 Ma calc-alkaline rocks in the Pilbara Archaean: isotopic and geochemical constraints from the Shaw Batholith. *Precambrian Res.* **60**, 117–149 (1993).

72. R. H. Smithies, D. C. Champion, K. F. Cassidy, Formation of Earth ' s early Archaean continental crust. **127**, 89–101 (2003).

73. M. T. D. Wingate, Ion microprobe baddeleyite and zircon ages for Late Archaean mafic dykes of the Pilbara Craton, Western Australia. *Aust. J. Earth Sci.* **46**, 493–500 (1999).

74. M. J. Bickle, *et al.*, A 3500 Ma Plutonic and Volcanic Calc-Alkaline Province in the Archaean East Pilbara Block. *Contrib. to Mineral. Petrol.* **84**, 25–35 (1983).

75. S. G. Nielsen, J. A. Baker, E. J. Krogstad, Petrogenesis of an early Archaean (3.4 Ga) norite dyke, Isua, West Greenland: Evidence for early Archaean crustal recycling? *Precambrian Res.* **118**, 133–148 (2002).

76. A. P. Nutman, C. R. L. Friend, V. C. Bennett, V. R. MCGregor, Dating of the Ameralik dyke swarms of the Nuuk district, southern West Greenland: mafic intrusion events starting from c. 3510 Ma. *J. Geol. Soc. London.* **161**, 421–430 (2004).

77. Puchtel, *et al.*, Lithophile and siderophile element systematics of Earth's mantle at the Archean-Proterozoic boundary: Evidence from 2.4 Ga komatiites. *Geochim. Cosmochim. Acta* **180**, 227–255 (2016).

78. Puchtel, J. Blichert-Toft, M. Touboul, M. F. Horan, R. J. Walker, The coupled 182W-142Nd record of early terrestrial mantle differentiation. *Geochemistry Geophys. Geosystems* **17**, 2168–2193 (2016).

79. M. Willbold, S. J. Mojzsis, H. W. Chen, T. Elliott, Tungsten isotope composition of the Acasta Gneiss Complex. *Earth Planet. Sci. Lett.* **419**, 168–177 (2015).

80. C. W. Dale, T. S. Kruijer, K. W. Burton, Highly siderophile element and 182W evidence for a partial late veneer in the source of 3.8 Ga rocks from Isua, Greenland. *Earth Planet. Sci. Lett.* **458**, 394–404 (2017).

81. D. L. Cook, M. Schönbächler, High-precision measurement of W isotopes in Fe–Ni alloy and the effects from the nuclear field shift. *J. Anal. At. Spectrom.* (2016) https:/doi.org/10.1039/C6JA00015K.